Role of UCHL1 in axonal injury and functional recovery after cerebral ischemia

Hao Liu[a,b,1], Nadya Povysheva[c,1], Marie E. Rose[a,b], Zhiping Mi[a,b], Joseph S. Banton[b], Wenjin Li[b], Fenghua Chen[b], Daniel P. Reay[a,b], Germán Barrionuevo[c], Feng Zhang[a,b,2], and Steven H. Graham[a,b,2]

[a]Geriatric Research Educational and Clinical Center, Veterans Affairs Pittsburgh Healthcare System, Pittsburgh, PA 15240; [b]Department of Neurology, University of Pittsburgh School of Medicine, Pittsburgh, PA 15213; and [c]Department of Neuroscience, University of Pittsburgh, Pittsburgh, PA 15260

Edited by Gregg L. Semenza, Johns Hopkins University School of Medicine, Baltimore, MD, and approved January 14, 2019 (received for review December 17, 2018)

Ubiquitin C-terminal hydrolase L1 (UCHL1) is a unique brain-specific deubiquitinating enzyme. Mutations in and aberrant function of UCHL1 have been linked to many neurological disorders. UCHL1 activity protects neurons from hypoxic injury, and binding of stroke-induced reactive lipid species to the cysteine 152 (C152) of UCHL1 unfolds the protein and disrupts its function. To investigate the role of UCHL1 and its adduction by reactive lipids in inhibiting repair and recovery of function following ischemic injury, a knock-in (KI) mouse expressing the UCHL1 C152A mutation was generated. Neurons derived from KI mice had less cell death and neurite injury after hypoxia. UCHL1 C152A KI and WT mice underwent middle cerebral artery occlusion (MCAO) or sham surgery. White matter injury was significantly decreased in KI compared with WT mice 7 d after MCAO. Histological analysis revealed decreased tissue loss at 21 d after injury in KI mice. There was also significantly improved sensorimotor recovery in postischemic KI mice. K63- and K48-linked polyubiquitinated proteins were increased in penumbra of WT mouse brains but not in KI mouse brains at 24 h post MCAO. The UCHL1 C152A mutation preserved excitatory synaptic drive to pyramidal neurons and their excitability in the periinfarct zone; axonal conduction velocity recovered by 21 d post MCAO in KI mice in corpus callosum. These results demonstrate that UCHL1 activity is an important determinant of function after ischemia and further demonstrate that the C152 site of UCHL1 plays a significant role in functional recovery after stroke.

UCHL1 | ischemia | axonal injury | electrophysiology | ubiquitin–proteasome pathway

Neuroprotective strategies that target excitotoxicity and other hyperacute mechanisms have not been successfully translated into effective therapies for stroke. Furthermore, many neuroprotective strategies target neuronal cell death mechanisms but do not address injury to axons and myelin (1–3). New approaches targeting delayed repair and recovery mechanisms and white matter injury are needed.

Ubiquitin C-terminal hydrolase L1 (UCHL1) is a multifunctional protein that is selectively expressed in neurons throughout the brain at high levels (4). UCHL1 may play an important role in repair of axons and neurons after injury by removal of abnormal proteins by the ubiquitin–proteasome pathway (UPP) and autophagy (5–8). UCHL1 closely interacts with proteins of the neuronal cytoskeleton and may play an important role in axonal transport and maintaining axonal integrity (9–11). UCHL1 also regulates synaptic function and long-term potentiation (LTP) and may be involved in memory function (12, 13). Mutations in UCHL1 result in axonal pathology and extensive deficits in motor function. Preservation of axonal integrity and synaptic function may play a pivotal role in restoration of motor and cognitive function after stroke (14). UCHL1 activity protects primary neurons from hypoxia-induced cell death (15).

Reactive lipids such as cyclopentenone prostaglandins (CyPgs) are produced after cerebral ischemia and may exacerbate injury and impede recovery via inhibition of the UPP (15–18). CyPgs bind to UCHL1 at cysteine 152 (C152), unfold the enzyme, and inhibit its function (19). Our recent work (11) has shown that the intrinsic hydrolase activity of the recombinant UCHL1 C152A mutant protein is similar to that of WT UCHL1 protein. However, hydrolase activity in the UCHL1 C152A mutant protein was better preserved after CyPg treatment compared with the WT protein. The UCHL1 C152A mutation ameliorates axonal pathology produced by treatment of primary neurons with CyPgs (11). To determine if binding of reactive lipids such as CyPgs to the C152 site is important in axonal injury, synaptic function, and behavioral outcome in stroke, we subjected knock-in (KI) mice bearing a C152A mutation and WT controls to middle cerebral artery occlusion (MCAO). The effect of the C152A mutation on UPP function, axonal conduction, synaptic function, neuronal excitability, and histological and behavioral outcomes after MCAO was determined.

Results

The UCHL1 C152A Mutation Protects Primary Neurons Against Hypoxia-Induced Cell Death, Axonal Injury, and Functional Deficits. To assess the effect of the UCHL1 C152A mutation on cell death induced by hypoxia/ischemia in vitro, primary neurons derived from WT

Significance

Many neuroprotective strategies have failed to translate to clinical trials, perhaps because of a failure to preserve white matter function. Ubiquitin C-terminal hydrolase L1 (UCHL1), a neuron-specific protein essential for axonal function, is deactivated by reactive lipids produced after cerebral ischemia. Mutation of the cysteine residue 152-reactive lipid-binding site of UCHL1 decreased axonal injury after hypoxia and ischemia in vitro and in vivo, preserved axonal conductance and synaptic function, and improved motor behavior after ischemia in mice. These results suggest that UCHL1 may play an important role in maintaining axonal function after cerebral ischemia. Restoration of UCHL1 activity or prevention of degradation of UCHL1 activity by preventing binding of substrates to cysteine residue 152 could be useful approaches for treatment of stroke.

Author contributions: H.L., N.P., Z.M., G.B., F.Z., and S.H.G. designed research; H.L., N.P., M.E.R., Z.M., J.S.B., W.L., F.C., D.P.R., and F.Z. performed research; H.L., N.P., M.E.R., Z.M., F.Z., and S.H.G. analyzed data; and H.L., N.P., M.E.R., Z.M., F.Z., and S.H.G. wrote the paper.

The authors declare no conflict of interest.

This article is a PNAS Direct Submission.

Data deposition: Data related to this work are available on figshare (https://doi.org/10.6084/m9.figshare.7651916).

[1]H.L. and N.P. contributed equally to this work.

[2]To whom correspondence may be addressed. Email: zhanfx2@upmc.edu or sgra@pitt.edu.

This article contains supporting information online at www.pnas.org/lookup/suppl/doi:10.1073/pnas.1821282116/-/DCSupplemental.

Published online February 13, 2019.

or UCHL1 C152A KI mice were subjected to oxygen/glucose deprivation (OGD) or hypoxia. Cell viability was measured 24 h after OGD or hypoxia by using the WST-1 assay and propidium iodide (PI) staining. As shown in Fig. 1 *A* and *B*, viability of UCHL1 C152A KI neurons was significantly greater than WT neurons 24 h after hypoxia and OGD. Next, the role of the UCHL1 C152A mutation on hypoxia-induced axonal injury was measured 24 h after hypoxia or normoxia. Hypoxia induced significant neurite damage as indicated by increased neurite fragments and decreased the number of intact neurites. This damage was significantly diminished in primary neurons from KI mice compared with WT (Fig. 1*C*). Thus, the C152A mutation protected neurites and neuronal cell bodies from injury.

To determine if the UCHL1 C152A mutation protects neurons from ischemia in vivo, WT and KI mice were subjected to 60 min MCAO and killed 21 d post injury. Tissue loss was significantly smaller in KI mice compared with WT controls ($16.62 \pm 3.45\%$ vs. $29.75 \pm 2.34\%$, $P < 0.01$; Fig. 1*E*). Short-term functional assessment was performed on post injury days (PIDs) 1–5 with four-limb symmetry and forelimb outstretch measures; long-term functional assessment was performed by using the cylinder test on PID 20–23. KI mice exhibited smaller functional deficits than WT mice in four-limb symmetry and forelimb outstretch measures, suggesting better short-term motor function in KI mice after cerebral ischemia. There was no significant difference between KI and WT mice with the sham surgery procedure. Long-term functional deficits were attenuated in KI mice as demonstrated by improved performance in the cylinder test (Fig. 1*D*).

The UCHL1 C152A Mutation Preserves Myelin Integrity and Decreases Axonal Injury After MCAO. White matter integrity in KI and WT mice was determined 7 d and 21 d after MCAO by immunodetection of myelin basic protein (MBP), a marker of myelin integrity, and nonphosphorylated pathological neurofilaments (SMI-32), an index of axonal injury (14, 20). Fluorescence intensities of MBP and SMI-32 were not significantly different between sham-operated WT and KI mice; however, there was decreased MBP fluorescence and increased SMI-32 fluorescence in the ipsilateral corpus callosum (CC) of WT mice 7 d post MCAO compared with KI (Fig. 2*A*). Similar changes were also observed in SMI-32 expression at 21 d after MCAO (*SI Appendix*, Fig. S1). MBP in ipsilateral penumbra 7 d after MCAO was significantly decreased in WT mice compared with WT sham mice, but there was no significant difference between sham and MCAO in KI mice (Fig. 2*B*). MBP detected by immunoblot was significantly decreased 7 d after MCAO in WT mice compared with sham WT in ipsilateral penumbra; there was no significant difference in KI mice (Fig. 2*B*). These data support the hypothesis that the UCHL1 C152A mutation preserves myelin integrity and decreases axonal injury after cerebral ischemia.

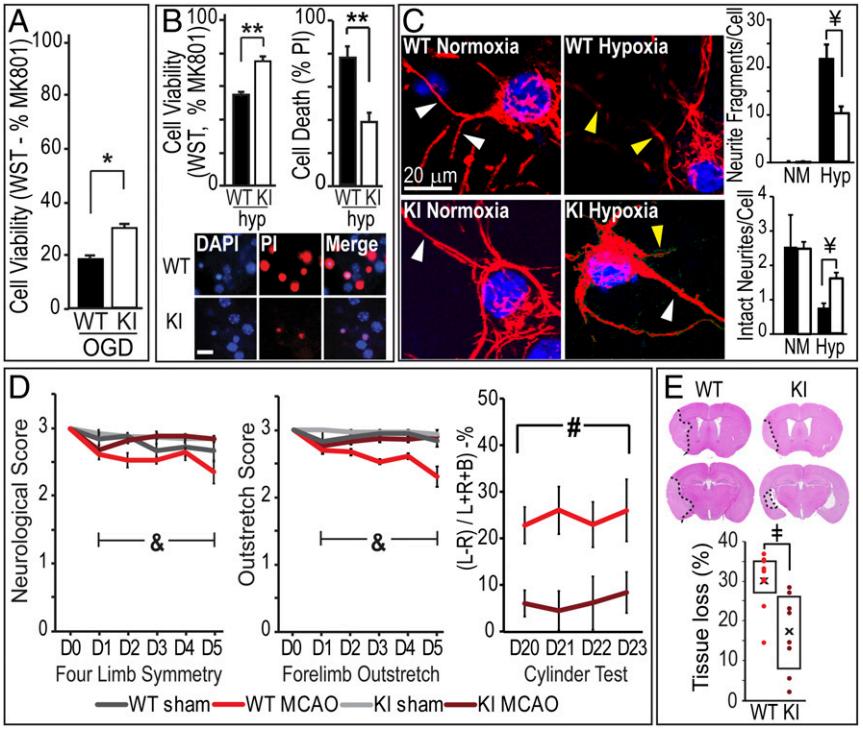

Fig. 1. The UCHL1 C152A mutation attenuates hypoxia/ischemia-induced neuronal injury and improves behavioral outcome. (*A* and *B*) In vitro cell viability and cell death in WT and mutant UCHL1 C152A (KI) primary neuronal culture after OGD (*A*) and hypoxia (*B*). (*A*) Cell viability based on WST-1 assay with MK801 (MK) as 100% survival control and staurosporine (SP; 30 μM) as 100% cell death control 24 h after 15 min OGD. Data are expressed as percent MK (n = 12 wells per group). (*B*, *Upper Left*) Cell viability 24 h after 3.5 h hypoxia based on WST-1 assay (n = 18 wells per group). (*B*, *Upper Right*) Cell death as measured by percent PI (red) or DAPI (blue) staining (n = 10 wells per group). (Scale bar: 20 μm.) (*C*) Effects of the C152A mutation on hypoxia-induced neurite damage. Primary neurons from WT or KI mice underwent 2.5 h hypoxia (Hyp) or normoxia (NM) treatment followed by immunohistochemical staining with anti-neurofilament (red) antibody. (*Left*) Representative confocal images. Yellow arrows indicate neurite fragments; white arrows are intact neurites. (*Right*) Fragment and intact neurite analysis 24 h post hypoxia (n = 8–15 fields per group). Blue indicates DAPI nuclear stain. (*D*) The UCHL1 C152A mutation attenuates behavioral deficits after 60 min MCAO. (*Left* and *Center*) Four-limb symmetry and forelimb outstretch scores on days 1–5 post ischemia. (*Right*) Cylinder test scores at days 20–23 post injury (L, ipsilateral; R, contralateral; B, both). (*E*) Whole-brain tissue loss in WT and KI mice 21 d post injury. (*Upper*) Representative H&E-stained slices. Dotted line indicates and infarct border. (*D* and *E*) n = 8–10 per group. Data are means ± SEM (*$P < 0.05$ and **$P < 0.01$, independent-samples t test; $^{¥}P < 0.001$, two-way ANOVA with Tamhane's T2 post hoc test; $^{\&}P < 0.001$, two-way repeated-measures ANOVA with Bonferroni post hoc test; $^{\#}P < 0.05$, ANOVA; $^{‡}P < 0.01$, Mann–Whitney U test). Black/gray bars indicate WT; white bars indicate KI.

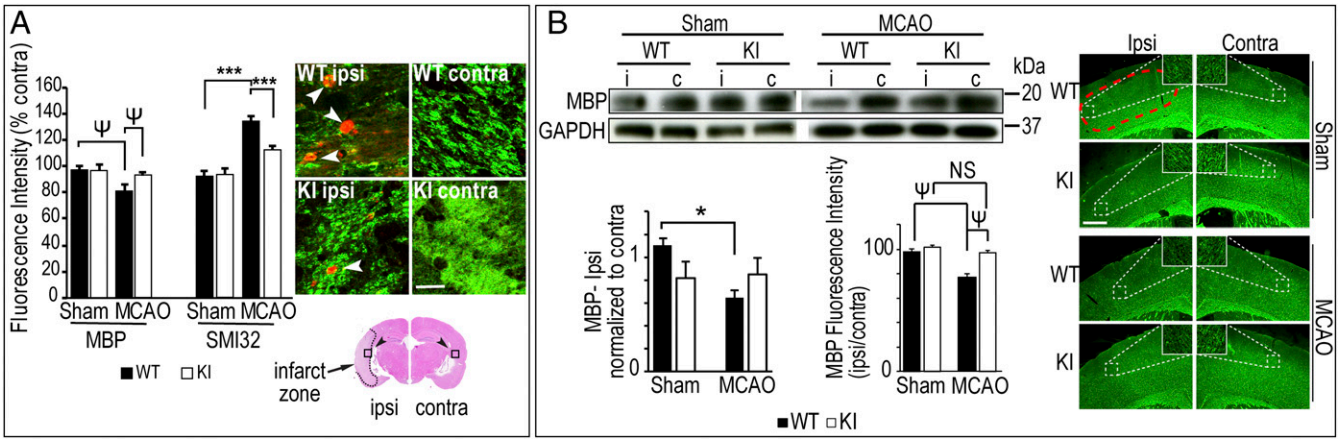

Fig. 2. The UCHL1 C152A mutation preserves white matter integrity and synaptic structure 7 d post ischemia. UCHL1 C152A KI and WT mice underwent 60 min MCAO or sham surgery. (*A*) White matter injury in CC. Brain slices at bregma −1.9 mm were immunostained by using anti-MBP (green) and anti-nonphosphorylated SMI-32 (red; at white arrows) antibodies. Fluorescence intensity was measured at infarct in ipsilateral (marked as "i") and contralateral ("c") CC (400 μm × 400 μm; black arrows; $n = 9$–10 per group). (Scale bar: 25 μm.) (*B*) Representative immunoblots and immunofluoromicrographs using anti-MBP antibody. (*Left*) Tissue lysates from penumbral cortex and densitometric analysis ($n = 7$–10 per group). (*Right*) MBP immunofluorescence intensity at penumbral cortex (area within red dashed line) at bregma 1.0 mm ($n = 9$–10 per group). (Scale bar: 500 μm.) Data are means ± SEM and are normalized to contralateral (*$P < 0.05$ and ***$P < 0.001$, two-way ANOVA with Tukey post hoc analysis; $^{\Psi}P < 0.05$, two-way ANOVA with Tamhane's T2 post hoc analysis). NS, not significant.

The UCHL1 C152A Mutation Preserves Axonal Conduction, Neuronal Excitability, and Synaptic Function After MCAO. The observation that the UCHL1 C152A mutation preserves MBP and decreases axonal injury as detected by SMI-32 antibody suggests that the mutation may also preserve axonal function after MCAO. Axonal function was assessed by measuring axonal conduction velocity in brain slices in CC. Significantly decreased conduction velocity in myelinated axons was observed at 7 d after MCAO compared with sham in WT and KI mice (Fig. 3*C*). MCAO also resulted in decreased conduction velocity for nonmyelinated axons on day 7 compared with sham in WT and KI mice (Fig. 3*C*). This decrease in axonal conduction velocity in myelinated and nonmyelinated axons persisted in WT mice but was mitigated in KI mice compared with sham 21 d post MCAO (Fig. 3*D*). Thus, axonal function recovered in KI mice after MCAO by 21 d, but not in WT mice.

To investigate the effects of the UCHL1 C152A mutation on neuronal activity in the periinfarct zone, intrinsic excitability of pyramidal neurons was assessed in WT and UCHL1 KI mice after MCAO or sham operation. Decreases in neuronal excitability could contribute to insufficient activation of pyramidal neurons and subsequent decline in the excitatory synaptic drive and thus further exacerbate the ischemic pathology. Pyramidal neurons exhibited lower frequency of firing produced by depolarizing current pulses 7 d post ischemia in WT mice compared with sham, but not on day 21 (Fig. 3*E*). In UCHL1 KI mice, no differences in firing frequency were observed between sham and MCAO conditions at day 7 or day 21 (Fig. 3 *E* and *F*). In addition, pyramidal neurons in WT mice exhibited higher action potential threshold on days 7 and 21 after MCAO compared with sham (Fig. 3*G*); action potential thresholds between sham and MCAO groups were unchanged in KI mice. These data indicate that the UCHL1 C152A mutation preserves excitability of pyramidal neurons after MCAO.

To assess excitatory synaptic drive in pyramidal neurons, the frequency and amplitude of the spontaneous excitatory postsynaptic currents (sEPSCs) in WT and KI mice were examined in slice preparations. Whereas amplitude of those events reflects possible changes on the postsynaptic site, their frequency might be indicative of the number of presynaptic terminals on those neurons. sEPSCs were recorded from pyramidal neurons identified by morphological and electrophysiological properties (*SI Appendix*, Fig. S3). MCAO resulted in decreased sEPSC frequency compared with sham on day 7 in WT mice, consistent with a decreased number of synaptic inputs; however, there was no difference in sEPSC frequency between sham and MCAO in KI mice (Fig. 3*I*). There were no significant differences in sEPSC amplitudes between groups. No significant differences were observed in sEPSC frequency in KI and WT mice at 21 d after MCAO (*SI Appendix*, Fig. S4*A*). In a similar fashion to the sEPSCs results, there was a decrease in miniature excitatory postsynaptic current (mEPSC) frequency 7 d post ischemia compared with sham animals in WT mice, but there were no significant differences between sham and MCAO in KI mice (Fig. 3*J*). By 21 d post ischemia, there was no difference in mEPSC frequency between sham and MCAO animals in WT or KI groups (*SI Appendix*, Fig. S4*B*). Amplitude of mEPSCs did not differ between MCAO and sham in WT or KI mice at 7 or 21 d post ischemia (Fig. 3*J* and *SI Appendix*, Fig. S4*B*). Taken together, these results are consistent with the hypothesis that the UCHL1 C152A mutation preserves synaptic function after ischemia.

The UCHL1 C152A Mutation Attenuates Polyubiquitinated Protein Accumulation and Autophagy Activation After MCAO. To detect the effects of the UCHL1 C152A mutation on ischemia-induced UPP function and autophagy, UCHL1, polyubiquitinated (poly-Ub) proteins, proteasome components, monoubiquitin, and autophagy markers beclin-1 and LC3B were detected in ipsilateral and contralateral penumbral cortex 24 h after MCAO by immunoblotting. The 20S proteasome activity was also measured 24 h post MCAO. There was increased accumulation of total poly-Ub proteins, UPP-independent K63-linked poly-Ub proteins, and K48-linked UPP-dependent poly-Ub proteins in WT mice compared with sham controls, but this effect was not found in KI mice. The ubiquitin monomer and UCHL1 proteins were unchanged after MCAO in WT and KI mice (Fig. 4). There were no differences in the expression of the proteasome subunits 19S and 20S (*SI Appendix*, Fig. S5*A*). The chymotrypsin-like 20S proteasome activity was significantly decreased in ipsilateral penumbra in WT mice 24 h after MCAO, but there was no significant difference between post-MCAO WT and KI groups (*SI Appendix*, Fig. S5*B*).

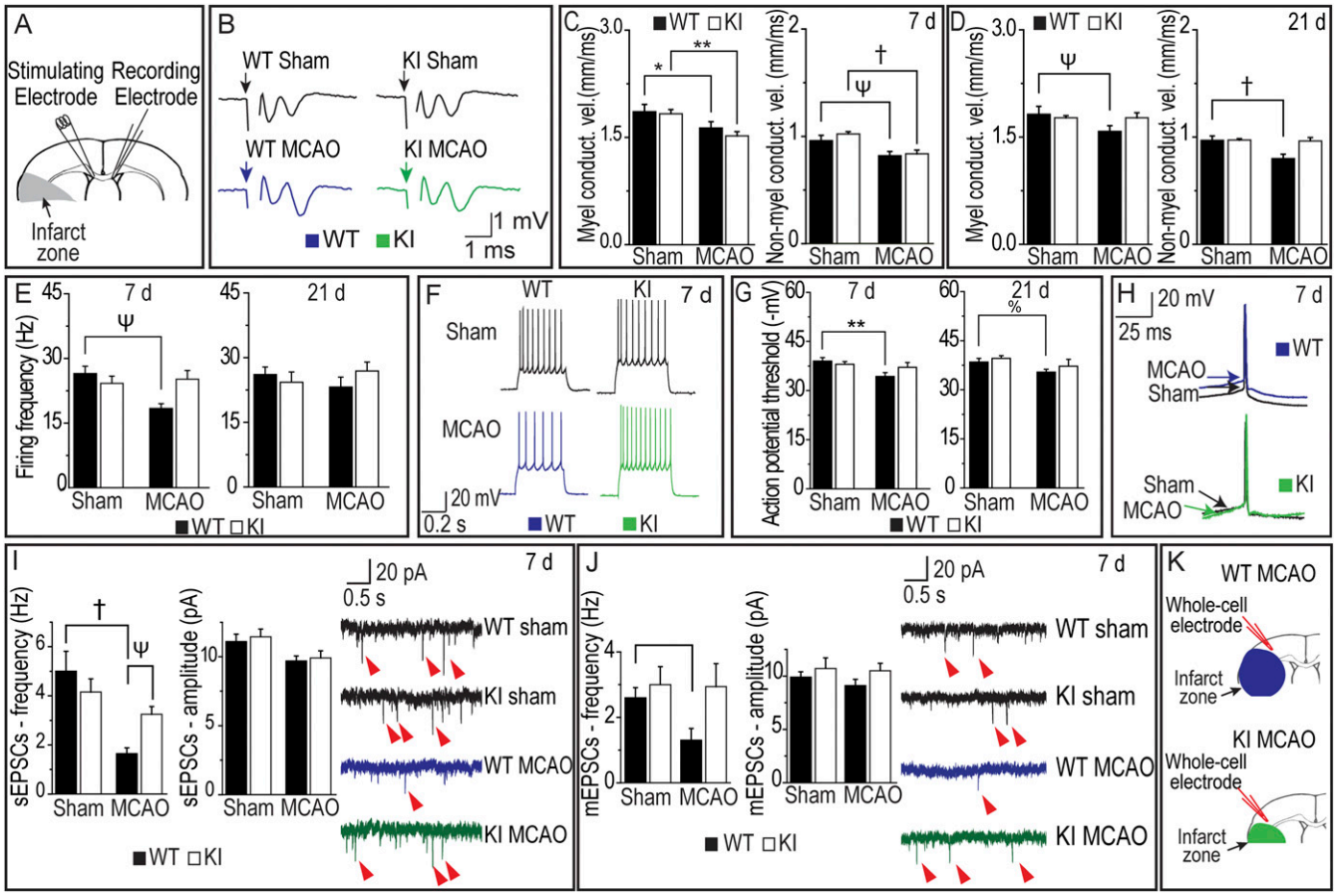

Fig. 3. (*A*) Position of stimulating and recording electrodes in CC for conduction velocity measurements in *B*–*D*. (*B*) Representative axonal activation recordings in CC. (*C* and *D*) Conduction velocity in myelinated and nonmyelinated fibers 7 d (*C*) and 21 d (*D*) post ischemia (n = 12–17 per group). (*E*) Firing frequency in sham and MCAO WT and UCHL1 mice 7 d and 21 d post ischemia (n = 10–14 per group). (*F*) Representative firing patterns of pyramidal neurons from mouse neocortex elicited by depolarizing current steps in WT (blue), KI (green), and sham surgery mice 7 d post ischemia. (*G*) Action potential threshold in 7 d (*Left*) and 21 d (*Right*) postischemic or sham surgery WT and KI mice (n = 10–13 per group). (*H*) Representative action potential at 7 d post ischemia in sham (black), MCAO WT (blue), and KI (green) mice. Arrows indicate action potential threshold. (*I*) sEPSC amplitude and frequency (*Left*) and representative recordings (*Right*) 7 d post ischemia with examples at red arrows (n = 9–11 per group). (*J*) mEPSCs at 7 d post ischemia with examples at red arrows (n = 6–9 per group). (*K*) Whole-cell electrode placement for sEPSC measurements in *I* and *J*. Data are means ± SEM (*P < 0.05 and **P < 0.01, two-way ANOVA with Tukey post hoc test; $^{\%}P$ <0.05, two-way ANOVA with least significant difference post hoc test; $^{\Psi}P$ < 0.05 and $^{\dagger}P$ < 0.01, two-way ANOVA with Tamhane's T2 post hoc testing). Black bars indicate WT; white bars indicate KI. Blue recording is WT MCAO; green recording is KI MCAO.

Impaired clearance of damaged proteins caused by compromised UPP function after brain ischemia may result in compensatory activation of autophagy. The ratio of LC3BII to LC3BI was significantly increased in ipsilateral penumbra in WT mice 24 h after MCAO, indicating activation of autophagy; this effect was not observed in KI mice (*SI Appendix*, Fig. S2). Another autophagy-related molecule, the Bcl2-interacting protein beclin-1, remained unchanged between WT and KI mice in MCAO and sham groups (*SI Appendix*, Fig. S2). These results indicate that activation of autophagy may occur through a beclin-1–independent mechanism.

Discussion

UCHL1 exhibits dual actions: it ligates ubiquitin onto proteins and hydrolyzes ubiquitin from proteins (8). UCHL1 has been shown to ligate K-48 and K-63 ubiquitin chains to proteins (8). Thus, UCHL1 has been proposed to be an important component of the UPP and has important signal-transduction effects in neurons. As the UPP is a crucial mechanism by which accumulations of abnormal proteins within neurons are degraded, UCHL1 may play an important role in removing abnormal protein aggregations within neurons after ischemia (15, 21, 22). In the present study, there was significantly less accumulation of K-48–linked poly-Ub proteins and a decrease in the ratio of LC3BII to LC3BI in ischemic cortex of KI mice compared with WT. These results suggest that the UCHL1 C152A mutation preserves UPP function and that activation of autophagy is not required to remove damaged proteins after stroke. Excessive amounts of ubiquitin proteins form protein aggregates within neurons after transient ischemia and have been hypothesized to result in the unfolded protein response and neuronal cell death (23). Thus, preservation of gray matter demonstrated by decreased tissue loss in the ischemic cortex of KI mice may be the result of preservation of UPP function.

Polymerization of ubiquitin at its lysine 63 (K-63) site is not associated with the UPP; rather, K-63 polyubiquitination has been shown to alter the structure and function of a host of proteins and has therefore been implicated in a variety of signal transduction and transport pathways (24). Therefore, UCHL1 may have functions in addition to protein degradation. The selective expression of UCHL1 in neurons suggests that it may have neuron-specific functions (21, 25–27). UCHL1 closely interacts with proteins of the neuronal cytoskeleton and may play an important role in axonal transport and maintaining axonal integrity (8, 12). Mutation or disruption of UCHL1 in mice leads to severe axonal pathology and

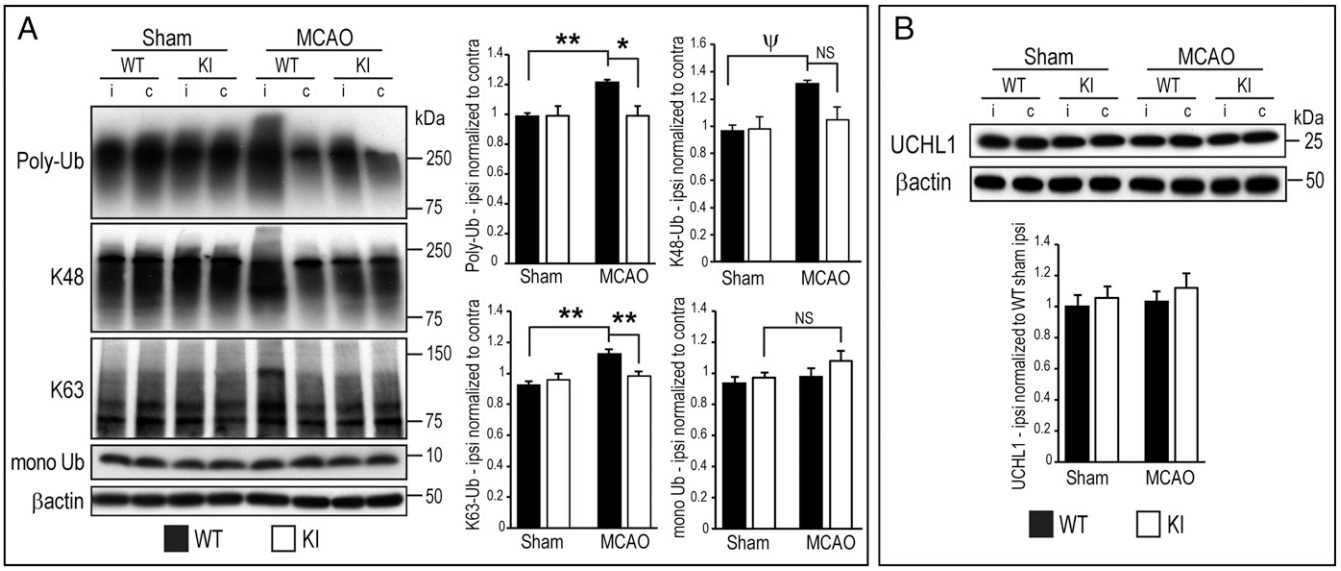

Fig. 4. UCHL1 C152A KI and WT mice underwent MCAO or sham surgery and were killed at 24 h post injury. Brain tissue lysates were prepared from ipsilateral (marked as "i") and contralateral ("c") cortical penumbral samples. (*A*, *Left*) Representative immunoblots of lysates probed with anti–poly-Ub, poly-Ub K48 (K48), poly-Ub K63 (K63), and monoubiquitinated (mono Ub) antibodies. (*A*, *Right*) Densitometric analysis of immunoblots normalized to respective contralateral tissue lysate. (*B*, *Upper*) Immunoblot of lysates probed with anti-UCHL1 antibody. (*B*, *Lower*) Densitometric analysis of immunoblots of ipsilateral normalized to WT sham ipsilateral (n = 8–10 per group; $^{*}P < 0.05$ and $^{**}P < 0.01$, two-way ANOVA with Bonferroni post hoc testing; $^{\Psi}P < 0.05$, two-way ANOVA with Tamhane's T2 post hoc testing). NS, not significant. Data are means ± SEM, with β-actin as loading control.

synaptic dysfunction (28). A mutation in UCHL1 produces gracile axonal dystrophy (GAD) characterized by axonal degeneration and spheroid formation and dying-back–type axonal degeneration (29). GAD mice have extensive sensory ataxia followed by progressive motor paresis (30, 31). Loss of UCHL1 function caused by a missense mutation in humans (UCHL1 E7A) leads to early-onset progressive neurodegeneration characterized by childhood-onset blindness, cerebellar ataxia, nystagmus, dorsal column dysfunction, and spasticity with upper motor neuron dysfunction (6). UCHL1 also regulates synaptic function and LTP under normal and pathological conditions and may play an important role in memory (13). UCHL1-null mice have abnormal synaptic transmission at the neuromuscular junction and accumulation of tubulovesicular structures at the presynaptic nerve terminals (6, 7). UCHL1-null mice exhibit neurodegeneration with progressive motor impairment and pathology in dendritic spines of the corticospinal neurons (31–33). These and other findings suggest that UCHL1 may play a major role in maintaining axonal transport and synaptic function and is essential in maintaining normal motor function (13, 34, 35).

In the present study, we found that there is increased detection of K-63 Ub-proteins 24 h after MCAO in WT mice, but no significant increase in K-63 Ub-proteins in KI mice. These finding are in contrast to the observation that UCHL1 dimerization-dependent ligase activity results in K-63 polyubiquitination of α-synuclein in vitro (8); however, the role of UCHL1 dimers in vivo is uncertain (36). The finding in the present study is consistent with the observation that UCHL1 inhibition increases accumulation of K63-linked Ub-proteins in tissue, perhaps as a result of loss of UCHL1 hydrolase activity (37). There were no differences in expression of UCHL1 between WT and KI in sham vs. MCAO mice. Thus, the increased detection of K-48 and K-63 poly-Ub proteins is consistent with a decreased activity of UCHL1 after ischemia, in keeping with inactivation of the enzyme by binding of reactive lipids to the C152 site on UCHL1.

Many neuroprotective strategies have been developed that target exclusively neuronal cell death mechanisms and gray matter injury, but none have succeeded in clinical trials (38). One hypothesis for this failure of translation is that stroke also produces extensive white matter injury by distinct mechanisms (1). There is increasing evidence that long-term behavioral outcome may be more dependent on white matter function than selective neuronal cell death (39). Stroke has been shown to produce substantial degradation in axonal function that can lead to a complete loss of conduction in axons (40). These pathological alterations in axons can be the result of damage of oligodendrocytes produced by ischemia or by damage to axons themselves (41–43) and are not reversed by therapies that target neuron-specific mechanisms.

The present data support an important role for UCHL1 in maintaining the integrity and recovery of function of axons after cerebral ischemia. UCHL1 C152A KI mice exhibited significantly less axonal injury vs. WT after MCAO as detected by SMI-32 antibody. There was also significantly less loss of myelin detected by MBP immunohistochemistry in mice bearing the C152A mutation. In keeping with these data, conduction velocity in the CC of KI mice was significantly greater than WT controls 7 d after MCAO. By 21 d after ischemia, conduction velocity in KI CC was not significantly different from sham controls, but there was persistent reduction in velocity in WT CC after MCAO compared with sham controls. Taken together, these results suggest that white matter injury is attenuated by the C152A mutation in UCHL1 and that UCHL1 may play an important role in preserving axonal function and promoting axonal recovery after ischemia.

Firing activity of neurons in the postischemic brain may be affected by the changes of the intrinsic membrane properties. Previous studies have shown that expression of intrinsic ion channels in neurons are down-regulated after ischemia (44–47). In the present report, there were changes in excitability of layer 2/3 pyramidal neurons in the periinfarct zone. Importantly, the UCHL1 mutation helped to preserve excitability of neurons, as no changes in firing frequency or action potential threshold were observed in KI mice at 7 d and 21 d post ischemia. A decrease in excitability of periinfarct pyramidal neurons might exacerbate the decrease in synaptic excitation observed in those neurons,

shutting down neuronal activity critically important for postischemic recovery (48). Because UCHL1 may regulate protein stability in a variety of neuronal proteins through the UPP, it may also be important in preserving normal intrinsic excitability of neurons in addition to axonal and synaptic function.

Axonal injury may also lead to a decrease in synaptic function and neuronal activity by decreasing the number of functional synaptic inputs to neurons. Immediately after stroke, there is an acute decrease in neuronal activity in the periinfarct zone that may be caused by reduction in excitatory inputs (49, 50). In the following days and weeks, synaptogenesis and restoration of axonal function in the periinfarct zone may result in recovery of synaptic function and restoration of normal neuronal activity (51, 52). Increased excitatory signaling has been detected as early as 3–7 d after stroke (53, 54). An increase in evoked EPSPs in periinfarct zones has been observed as early as 5 d after stroke (48). In the present study, there were deficits in excitatory signaling in the periinfarct cortex in WT mice after ischemia: frequency of sEPSCs and mEPSCs was decreased 7 d after MCAO. Reduction in sEPSC and mEPSC frequency may result from a reduction in the number of excitatory inputs. The loss of excitatory inputs is likely caused by loss of axonal terminals as a result of axonal damage or death of neuronal cell bodies in gray matter. These changes may hinder recovery by thwarting plasticity associated with glutamatergic synapses. The EPSC data from KI mice indicate that the UCHL1 C152A mutation is responsible for preservation or more efficient recovery of synaptic function in mice bearing this mutation.

Restoration of axonal integrity, synapses, and intrinsic neuronal properties may underlie recovery of function after stroke. In the present study, postischemic mice bearing the C152A mutation had improved short-term motor function as measured by four-limb symmetry and forelimb outstretch tests and improved long-term motor behavior observed in the cylinder test compared with postischemic WT mice. Thus, preserved axonal integrity and synaptic function in mice bearing the UCHL1 C152A mutation are associated with improved motor recovery, suggesting that these mechanisms are important determinants of long-term functional outcome.

The mechanisms that underlie recovery of function after stroke are complex and interdependent, and it is therefore difficult to ascertain from these data how much of the observed improvements in electrophysiological and behavioral recovery are the results of acute neuroprotective effects vs. more robust recovery mechanisms. Additional studies with in vitro models are needed to address the role of UCHL1 in repair and recovery mechanisms.

White matter injury is an important cause of disability after stroke, but there are few therapeutic strategies available that target its preservation (1). Results from this study demonstrate that mutation of the UCHL1 C152 site reduces damage to gray and white matter, resulting in recovery of motor function after MCAO. These findings support the hypothesis that UCHL1 activity plays an important role in ischemic neuronal injury and preserving axonal function after stroke, and that binding of substrates to the C152 site of UCHL1 is important in the pathophysiology of injury and recovery. Inhibition of substrate binding to the C152 site or augmentation of expression of UCHL1 after stroke could be useful strategies to preserve gray and white matter and improve functional outcome after stroke.

Materials and Methods

Generation of the UCHL1 C152A KI Mouse. The BAC technique was used to construct a UCHL1 C152A KI mouse as previously described (11). Animal studies were performed in accordance with the recommendations in the *Guide for the Care and Use of Laboratory Animals* of the National Institutes of Health (55). The protocol was approved by the University of Pittsburgh Institutional Animal Care and Use Committee (protocol no. IS00001941).

Cortical Primary Neuron-Enriched Culture from WT and UCHL1 C152A KI Mice. Mouse cortical primary neuronal cultures were prepared from embryonic day 17 fetal WT or KI mice as previously described and used for experiments after 9 days in vitro (17). Cells from the same genotype were pooled before plating and grown in serum-free Neurobasal medium (Invitrogen) supplemented with B27 and GlutaMAX (Invitrogen).

In Vitro Axonal Injury Analysis. In vitro axonal injury analysis was performed as described previously with minor modifications (11). Axon degeneration quantification was performed by a blinded investigator as described previously (56, 57).

MCAO. MCAO was induced in WT and KI male mice by making a midline incision at the trachea, retracting soft tissues, and advancing a silicon-coated nylon suture into the MCA for a duration of 60 min, as previously described with some modifications, by a surgeon blinded to the genotype of the mice (58). Core infarct and penumbral brain tissues were rapidly dissected and frozen or perfusion-fixed at 24 h, 7 d, and 21 d for analysis by immunoblotting or immunohistochemistry (n = 7–10 per group). Mice undergoing sham surgery were used as controls. Outcome measurements were made by observers unaware of the experimental group.

Behavioral Assessment. Mouse four-limb symmetry and forelimb outstretch testing was performed by using methods established by Garcia et al. (59). Cylinder testing was performed by using methods outlined by Schallert et al. (60) and Hua et al. (61). Test results were video recorded for analysis by an investigator blinded to the group.

Brain Tissue Loss Measurement. Mice were euthanized at 21 d after MCAO or sham surgery by using CO_2, followed by brain perfusion fixation with 4% paraformaldehyde. Brains were embedded in paraffin, cut at 7 μm, and stained with H&E. The method of Kim et al. was used to quantify tissue loss (62). Tissue loss is calculated by subtracting surviving gray matter volume in lesioned hemispheres from gray matter volumes in unlesioned hemispheres and is expressed as percent unlesioned gray matter volume (63). ImageJ version 1.50i (National Institutes of Health) was used to measure all areas to avoid bias.

Electrophysiological Recordings. Whole-cell recordings were made from pyramidal neurons in layers 2–3 of the mouse neocortex located ∼1 mm from the edge of the infarct visualized by IR differential interference contrast videomicroscopy by using a Zeiss Axioskop microscope (Carl Zeiss) with a 40× water immersion objective and a digital video camera (CoolSnap; Photometrics). Voltage and current recordings were performed with a MultiClamp 700A amplifier in bridge-balance mode (Axon Instruments).

Assessment of Excitatory Inputs. sEPSCs were recorded at a holding potential of −70 mV. mEPSCs were recorded at a holding potential of −70 mV in the presence of tetrodotoxin to inhibit action potential-mediated excitatory postsynaptic currents. Spontaneous and miniature events were analyzed by using the MiniAnalysis program (Synaptosoft).

Analysis of Intrinsic Membrane Properties. Membrane properties of neurons were analyzed by using Clampfit 10.2 software (Molecular Devices).

Estimation of Axonal Conduction Velocity. Compound action potentials (CAPs) were evoked from the CC (64, 65). A stimulating electrode was placed ipsilateral to the MCAO-affected area, and a recording electrode was placed contralateral to the MCAO site (Fig. 3*C*). We used the approach by Reeves et al. (65) that enabled separate quantification of CAPs generated by two populations of callosal axons. Axonal conduction velocity was estimated as the ratio of the distance between recording and stimulating electrodes and the time between the onset of stimulation and the first negative peak for myelinated fiber response and the second peak for unmyelinated fiber response.

Proteasome Activity Assay. Chymotrypsin-like activity of the 20S proteasome was measured in WT and UCHL1 C152A KI mice 24 h after MCAO or sham surgery. Fluorogenic substrate Suc-[Leu-Leu-Val-Tyr (LLVY)]-7-amino-4-methylcoumarin cleavage was measured by using a fluorescence-based assay kit (APT280; Millipore Sigma) following the manufacturer's instructions.

Data Sharing. Reagents and model organisms will be made available to other researchers via applicable material transfer agreements and/or licensing agreements. Data related to this work are available on figshare (https://doi.org/10.6084/m9.figshare.7651916).

Statistical Analysis. Data sets were examined for normality and equal variance before statistical analysis, and outliers were removed as determined by using 1.5× interquartile range (SPSS version 24; IBM). Data are expressed as means ± SEM and were analyzed by using two-way ANOVA with Tukey (equal variances) or Tamhane's T2 (unequal variances) post hoc testing unless otherwise noted. Cell viability was analyzed by using an independent-samples *t* test, and brain tissue loss was analyzed with the nonparametric Mann–Whitney *U* test. Results were considered significant at $P < 0.05$.

SI Appendix, Materials and Methods provides additional details regarding the study methods.

ACKNOWLEDGMENTS. This work was supported by National Institutes of Health/National Institute of Neurological Disorders and Stroke Grant 2R01NS037459-14A1 (to S.H.G.). The contents do not represent the views of the Department of Veterans Affairs or the United States Government.

1. Wang Y, et al. (2016) White matter injury in ischemic stroke. *Prog Neurobiol* 141:45–60.
2. Jiang X, et al. (2016) A post-stroke therapeutic regimen with omega-3 polyunsaturated fatty acids that promotes white matter integrity and beneficial microglial responses after cerebral ischemia. *Transl Stroke Res* 7:548–561.
3. Stetler RA, et al. (2016) APE1/Ref-1 facilitates recovery of gray and white matter and neurological function after mild stroke injury. *Proc Natl Acad Sci USA* 113:E3558–E3567.
4. Larsen CN, Price JS, Wilkinson KD (1996) Substrate binding and catalysis by ubiquitin C-terminal hydrolases: Identification of two active site residues. *Biochemistry* 35:6735–6744.
5. Kabuta T, Wada K (2008) Insights into links between familial and sporadic Parkinson's disease: Physical relationship between UCH-L1 variants and chaperone-mediated autophagy. *Autophagy* 4:827–829.
6. Bilguvar K, et al. (2013) Recessive loss of function of the neuronal ubiquitin hydrolase UCHL1 leads to early-onset progressive neurodegeneration. *Proc Natl Acad Sci USA* 110:3489–3494.
7. Chen F, Sugiura Y, Myers KG, Liu Y, Lin W (2010) Ubiquitin carboxyl-terminal hydrolase L1 is required for maintaining the structure and function of the neuromuscular junction. *Proc Natl Acad Sci USA* 107:1636–1641.
8. Liu Y, Fallon L, Lashuel HA, Liu Z, Lansbury PT, Jr (2002) The UCH-L1 gene encodes two opposing enzymatic activities that affect alpha-synuclein degradation and Parkinson's disease susceptibility. *Cell* 111:209–218.
9. Bheda A, Gullapalli A, Caplow M, Pagano JS, Shackelford J (2010) Ubiquitin editing enzyme UCH L1 and microtubule dynamics: Implication in mitosis. *Cell Cycle* 9:980–994.
10. Pukaß K, Richter-Landsberg C (2015) Inhibition of UCH-L1 in oligodendroglial cells results in microtubule stabilization and prevents α-synuclein aggregate formation by activating the autophagic pathway: Implications for multiple system atrophy. *Front Cell Neurosci* 9:163.
11. Liu H, et al. (2015) The point mutation UCH-L1 C152A protects primary neurons against cyclopentenone prostaglandin-induced cytotoxicity: Implications for post-ischemic neuronal injury. *Cell Death Dis* 6:e1966.
12. Sakurai M, et al. (2008) Reduction in memory in passive avoidance learning, exploratory behaviour and synaptic plasticity in mice with a spontaneous deletion in the ubiquitin C-terminal hydrolase L1 gene. *Eur J Neurosci* 27:691–701.
13. Gong B, et al. (2006) Ubiquitin hydrolase Uch-L1 rescues beta-amyloid-induced decreases in synaptic function and contextual memory. *Cell* 126:775–788.
14. Suenaga J, et al. (2015) White matter injury and microglia/macrophage polarization are strongly linked with age-related long-term deficits in neurological function after stroke. *Exp Neurol* 272:109–119.
15. Liu H, et al. (2011) Modification of ubiquitin-C-terminal hydrolase-L1 by cyclopentenone prostaglandins exacerbates hypoxic injury. *Neurobiol Dis* 41:318–328.
16. Liu H, et al. (2013) Prostaglandin D2 toxicity in primary neurons is mediated through its bioactive cyclopentenone metabolites. *Neurotoxicology* 39:35–44.
17. Liu H, et al. (2013) Increased generation of cyclopentenone prostaglandins after brain ischemia and their role in aggregation of ubiquitinated proteins in neurons. *Neurotox Res* 24:191–204.
18. Figueiredo-Pereira ME, Rockwell P, Schmidt-Glenewinkel T, Serrano P (2015) Neuroinflammation and J2 prostaglandins: Linking impairment of the ubiquitin-proteasome pathway and mitochondria to neurodegeneration. *Front Mol Neurosci* 7:104.
19. Koharudin LM, et al. (2010) Cyclopentenone prostaglandin-induced unfolding and aggregation of the Parkinson disease-associated UCH-L1. *Proc Natl Acad Sci USA* 107:6835–6840.
20. Han L, et al. (2015) Rosiglitazone promotes white matter integrity and long-term functional recovery after focal cerebral ischemia. *Stroke* 46:2628–2636.
21. Graham SH, Liu H (2017) Life and death in the trash heap: The ubiquitin proteasome pathway and UCHL1 in brain aging, neurodegenerative disease and cerebral Ischemia. *Ageing Res Rev* 34:30–38.
22. Shen H, Sikorska M, Leblanc J, Walker PR, Liu QY (2006) Oxidative stress regulated expression of ubiquitin carboxyl-terminal hydrolase-L1: Role in cell survival. *Apoptosis* 11:1049–1059.
23. Hu BR, Martone ME, Jones YZ, Liu CL (2000) Protein aggregation after transient cerebral ischemia. *J Neurosci* 20:3191–3199.
24. Chen ZJ, Sun LJ (2009) Nonproteolytic functions of ubiquitin in cell signaling. *Mol Cell* 33:275–286.
25. Kabuta T, Furuta A, Aoki S, Furuta K, Wada K (2008) Aberrant interaction between Parkinson disease-associated mutant UCH-L1 and the lysosomal receptor for chaperone-mediated autophagy. *J Biol Chem* 283:23731–23738.
26. Osaka H, et al. (2003) Ubiquitin carboxy-terminal hydrolase L1 binds to and stabilizes monoubiquitin in neuron. *Hum Mol Genet* 12:1945–1958.
27. Sakurai M, et al. (2006) Ubiquitin C-terminal hydrolase L1 regulates the morphology of neural progenitor cells and modulates their differentiation. *J Cell Sci* 119:162–171.
28. Gong B, Radulovic M, Figueiredo-Pereira ME, Cardozo C (2016) The ubiquitin-proteasome system: Potential therapeutic targets for alzheimer's disease and spinal cord injury. *Front Mol Neurosci* 9:4.
29. Yamazaki K, et al. (1988) Gracile axonal dystrophy (GAD), a new neurological mutant in the mouse. *Proc Soc Exp Biol Med* 187:209–215.
30. Kikuchi T, Mukoyama M, Yamazaki K, Moriya H (1990) Axonal degeneration of ascending sensory neurons in gracile axonal dystrophy mutant mouse. *Acta Neuropathol* 80:145–151.
31. Saigoh K, et al. (1999) Intragenic deletion in the gene encoding ubiquitin carboxy-terminal hydrolase in gad mice. *Nat Genet* 23:47–51.
32. Goto A, et al. (2009) Proteomic and histochemical analysis of proteins involved in the dying-back-type of axonal degeneration in the gracile axonal dystrophy (gad) mouse. *Neurochem Int* 54:330–338.
33. Miura H, et al. (1993) Progressive degeneration of motor nerve terminals in GAD mutant mouse with hereditary sensory axonopathy. *Neuropathol Appl Neurobiol* 19:41–51.
34. Genç B, et al. (2016) Absence of UCHL 1 function leads to selective motor neuropathy. *Ann Clin Transl Neurol* 3:331–345.
35. Jara JH, et al. (2015) Corticospinal motor neurons are susceptible to increased ER stress and display profound degeneration in the absence of UCHL1 function. *Cereb Cortex* 25:4259–4272.
36. Das C, et al. (2006) Structural basis for conformational plasticity of the Parkinson's disease-associated ubiquitin hydrolase UCH-L1. *Proc Natl Acad Sci USA* 103:4675–4680.
37. Susor A, et al. (2010) Role of ubiquitin C-terminal hydrolase-L1 in antipolyspermy defense of mammalian oocytes. *Biol Reprod* 82:1151–1161.
38. Savitz SI, Baron JC, Yenari MA, Sanossian N, Fisher M (2017) Reconsidering neuroprotection in the reperfusion Era. *Stroke* 48:3413–3419.
39. Goldberg MP, Ransom BR (2003) New light on white matter. *Stroke* 34:330–332.
40. Baltan S (2016) Age-specific localization of NMDA receptors on oligodendrocytes dictates axon function recovery after ischemia. *Neuropharmacology* 110:626–632.
41. Mifsud G, Zammit C, Muscat R, Di Giovanni G, Valentino M (2014) Oligodendrocyte pathophysiology and treatment strategies in cerebral ischemia. *CNS Neurosci Ther* 20:603–612.
42. Shi H, et al. (2015) Demyelination as a rational therapeutic target for ischemic or traumatic brain injury. *Exp Neurol* 272:17–25.
43. Shindo A, et al. (2016) Subcortical ischemic vascular disease: Roles of oligodendrocyte function in experimental models of subcortical white-matter injury. *J Cereb Blood Flow Metab* 36:187–198.
44. Aarts M, et al. (2003) A key role for TRPM7 channels in anoxic neuronal death. *Cell* 115:863–877.
45. Alim I, Teves L, Li R, Mori Y, Tymianski M (2013) Modulation of NMDAR subunit expression by TRPM2 channels regulates neuronal vulnerability to ischemic cell death. *J Neurosci* 33:17264–17277.
46. Lei Z, Zhang H, Liang Y, Xu ZC (2016) Reduced expression of IA channels is associated with post-ischemic seizures. *Epilepsy Res* 124:40–48.
47. Thompson RJ (2015) Pannexin channels and ischaemia. *J Physiol* 593:3463–3470.
48. Clarkson AN, et al. (2011) AMPA receptor-induced local brain-derived neurotrophic factor signaling mediates motor recovery after stroke. *J Neurosci* 31:3766–3775.
49. Dennis SH, et al. (2011) Oxygen/glucose deprivation induces a reduction in synaptic AMPA receptors on hippocampal CA3 neurons mediated by mGluR1 and adenosine A3 receptors. *J Neurosci* 31:11941–11952.
50. Murphy TH, Corbett D (2009) Plasticity during stroke recovery: From synapse to behaviour. *Nat Rev Neurosci* 10:861–872.
51. Cramer SC (2008) Repairing the human brain after stroke: I. Mechanisms of spontaneous recovery. *Ann Neurol* 63:272–287.
52. Stroemer RP, Kent TA, Hulsebosch CE (1998) Enhanced neocortical neural sprouting, synaptogenesis, and behavioral recovery with D-amphetamine therapy after neocortical infarction in rats. *Stroke* 29:2381–2393; discussion 2393–2385.
53. Centonze D, et al. (2007) Synaptic plasticity during recovery from permanent occlusion of the middle cerebral artery. *Neurobiol Dis* 27:44–53.
54. Pang ZP, Deng P, Ruan YW, Xu ZC (2002) Depression of fast excitatory synaptic transmission in large aspiny neurons of the neostriatum after transient forebrain ischemia. *J Neurosci* 22:10948–10957.
55. National Research Council (2011) *Guide for the Care and Use of Laboratory Animals* (National Academies Press, Washington, DC), 8th Ed.
56. Hosie KA, King AE, Blizzard CA, Vickers JC, Dickson TC (2012) Chronic excitotoxin-induced axon degeneration in a compartmented neuronal culture model. *ASN Neuro* 4:e00076.
57. Fang W, et al. (2015) Role of the Akt/GSK-3β/CRMP-2 pathway in axon degeneration of dopaminergic neurons resulting from MPP+ toxicity. *Brain Res* 1602:9–19.
58. Jing Z, et al. (2014) Neuronal NAMPT is released after cerebral ischemia and protects against white matter injury. *J Cereb Blood Flow Metab* 34:1613–1621.
59. Garcia JH, Wagner S, Liu KF, Hu XJ (1995) Neurological deficit and extent of neuronal necrosis attributable to middle cerebral artery occlusion in rats. Statistical validation. *Stroke* 26:627–634, discussion 635.
60. Hua Y, et al. (2002) Behavioral tests after intracerebral hemorrhage in the rat. *Stroke* 33:2478–2484.
61. Schallert T, Fleming SM, Leasure JL, Tillerson JL, Bland ST (2000) CNS plasticity and assessment of forelimb sensorimotor outcome in unilateral rat models of stroke, cortical ablation, parkinsonism and spinal cord injury. *Neuropharmacology* 39:777–787.

62. Kim E, et al. (2015) Daidzein augments cholesterol homeostasis via ApoE to promote functional recovery in chronic stroke. *J Neurosci* 35:15113–15126.
63. Ahmad M, Zhang Y, Liu H, Rose ME, Graham SH (2009) Prolonged opportunity for neuroprotection in experimental stroke with selective blockade of cyclooxygenase-2 activity. *Brain Res* 1279:168–173.
64. Baker AJ, et al. (2002) Attenuation of the electrophysiological function of the corpus callosum after fluid percussion injury in the rat. *J Neurotrauma* 19:587–599.
65. Reeves TM, Phillips LL, Povlishock JT (2005) Myelinated and unmyelinated axons of the corpus callosum differ in vulnerability and functional recovery following traumatic brain injury. *Exp Neurol* 196:126–137.